

TIME-DELAY AND DOPPLER ESTIMATION WITH A CARRIER MODULATED BY A BAND-LIMITED SIGNAL

Joan M. Bernabeu Frias^{1,2}, Lorenzo Ortega^{2,3}, Antoine Blais⁴, Yoan Gregoire⁵, Eric Chaumette¹

¹ ISAE-SUPAERO, ² T&SA, ³ IPSA, ⁴ ENAC, ⁵ CNES

ABSTRACT

Since time-delay and phase estimation is a fundamental task in a plethora of engineering fields, several CRB and MLE expressions have been derived for the past decades. In all these previous works, a common hypothesis is that the wave transmission process introduces an unknown phase which prevents from estimating both delay and transmission phase components. By revisiting this problem, including the derivation of the MLE and the associated CRB, we show that this well-admitted assertion is not true strictly: both informations can be estimated, but generally with a sub-optimal achievable MSE in the asymptotic region. Moreover, since practical problems exist where the transmission phase can be estimated apart, adding this additional measure to the observation model provides a setting allowing to explore the contribution of each signal component (carrier frequency, baseband signal and transmission phase measure) to the achievable MSE of time-delay and phase estimation in the asymptotic region.

Index Terms— Cramér-Rao bound, time-delay and phase estimation, band-limited signals.

1. INTRODUCTION

Time-delay and Doppler estimation appear in a plethora of engineering fields such as navigation, radar, reflectometry, sonar or communications, to name a few [1–9], being the estimation of such parameters a key first stage of the receiver [5, 8, 9]. For any of these applications, when designing and assessing estimation techniques, it is of fundamental importance to know the ultimate achievable performance in the mean squared error (MSE) sense, an information which can be brought by the Cramér-Rao bounds (CRB) [10], the most popular lower bound on the MSE, mainly due to its simplicity of calculation for various problems (see [4, §8.4] and [11, Part III]). In addition, the CRB gives an accurate estimation of the MSE of the maximum likelihood estimator (MLE), in the asymptotic region of operation and under certain conditions, i.e., in the large sample regime and/or high signal-to-noise (SNR) regime of the Gaussian conditional signal model (CSM) [12, 13]. So, it is not surprising that several CRB expressions for the delay-Doppler estimation problem have been derived for the past decades, for finite narrow-band signals [2, 14–22], finite wideband signals [14, 17, 20, 23–26] or infinite [27] bandwidth signals. In all these previous works, a common hypothesis is that the wave transmission process introduces an unknown phase component which prevents from exploiting the delay phase component from the carrier. This unknown phase component arises from the common hypothesis of an imperfect knowledge of the transmitter and/or receiver antenna (imperfect knowledge of the center of phase and/or the hyper-frequency electronics) and/or of the

radio-frequency electronics of transmitter and/or receiver. In such studies, all the phase components are grouped and combined with the amplitude component leading to an unknown complex amplitude. This is likely the reason why a thorough treatment of the case where such an unknown phase component does not exist seems to have been overlooked in the open literature. Hence the purpose of this communication, which provides a derivation of the MLE for the CSM (different from the commonly used one) and the associated CRB for the standard narrow-band signal model, which allows to explore the contribution of each signal component (carrier frequency and baseband signal) to the achievable MSE of time-delay and Doppler estimation in the asymptotic region. For such a scenario to occur, it is enough to consider a ground-based navigation scenario where the transmitter is static (an anchor) and the receiver (a tag) plans to move from a known location to another known location (way-points). At each known location, the receiver can estimate the phase component due to the transmission process and compensate for it during its motion towards the next known location.

The contents of the study have been structured in four sections. Section 2 presents the signal model and the associated MLE. The signal model employed is an instance of the CSM, which is known to be asymptotically efficient as the number of samples or the signal-to-noise ratio (SNR) increase [13]. Section 3 derives the CRB expressions for the proposed signal model, starting from the Slepian-Bangs formula [10]. Then, the Nyquist-Shannon theorem is applied under the assumption of a band-limited signal, which give way to a closed-form version of the CRB. The obtained CRB and Maximum-Likelihood Estimator equations are validated in Section 4 via Monte Carlo simulations. Next, the convergence of the MLE's MSE to the derived CRB is shown for certain SNR regimes, referred to as "Threshold". Finally, the key observations and contributions of the paper are collected in Section 5.

2. SIGNAL MODEL AND MLE

To define the signal model of interest, consider the line of sight of a band-limited signal $s(t)$ with bandwidth B over a carrier with frequency f_c from a transmitter T at position $\mathbf{P}_T(t)$ to a receiver R at position $\mathbf{P}_R(t)$. The distance travelled by the transmitted signal is $\mathbf{P}_{TR} = \|\mathbf{P}_T(t - \tau_0(t)) - \mathbf{P}_R(t)\| \approx \frac{(\mathbf{P}_T - \mathbf{P}_R)}{c} + \frac{v}{c}t$, that is, a first order approximation where we can redefine $\tau = \frac{(\mathbf{P}_T - \mathbf{P}_R)}{c}$, $b = \frac{v}{c}$ and with v the radial velocity. The narrowband received signal at the output of the Hilbert filter can be expressed as [28, 29]

$$x(t) = \alpha a(t - \tau) e^{-j2\pi f_c(\tau + b(t - \tau))} + n(t), \quad (1)$$

$$x(t) = \alpha a(t; \boldsymbol{\eta}) e^{j\varphi(t; \boldsymbol{\eta})} + n(t), \quad (2)$$

with $n(t)$ a complex circular white Gaussian noise with unknown variance σ_n^2 , α a real positive value which represents the amplitude,

This work was partially supported by CNES, IPSA and DGA/AID project 2021.65.0070.

$\varphi(\boldsymbol{\eta}) = -2\pi f_c(\tau + b(t - \tau))$ and $\boldsymbol{\eta} = [\tau, b]^T$. Note that this model differs from [28] since α is a real positive value and τ is included in the phase. Considering the acquisition of $N = N_2 - N_1 + 1$ samples at the sampling frequency $F_s = B = 1/T_s$, The discrete vector signal model yields to

$$\mathbf{x} = \alpha \mathbf{a}(\boldsymbol{\eta}) e^{j\varphi(\boldsymbol{\eta})} + \mathbf{n} \quad (3)$$

with $\boldsymbol{\epsilon} = (\sigma_n^2, \boldsymbol{\zeta})^T$ and $\boldsymbol{\zeta} = (\alpha, \boldsymbol{\eta})^T$ the vectors of unknown parameters. Note that this is a particular instantiation of the general conditionnal signal model (CSM) [30]. In the following, we denote $\mathbf{a}'(\boldsymbol{\eta}) = \mathbf{a}(\boldsymbol{\eta}) e^{j\varphi(\boldsymbol{\eta})}$ and the following rearrangement is considered

$$\underline{\mathbf{a}}'(\boldsymbol{\eta}) = (\Re \{ \mathbf{a}'(\boldsymbol{\eta}) \}, \Im \{ \mathbf{a}'(\boldsymbol{\eta}) \})^T, \quad (4)$$

$$\frac{\partial \underline{\mathbf{a}}'(\boldsymbol{\eta})}{\partial \boldsymbol{\eta}} = \left(\frac{\partial}{\partial \boldsymbol{\eta}} \Re \{ \mathbf{a}'(\boldsymbol{\eta}) \}, \frac{\partial}{\partial \boldsymbol{\eta}} \Im \{ \mathbf{a}'(\boldsymbol{\eta}) \} \right)^T, \quad (5)$$

where $\Re \{ \cdot \}$ and $\Im \{ \cdot \}$ represent the real and imaginary part of a complex number.

2.1. MLE with inequality constraint

The MLE is derived from the well known mean-squared error minimization procedure. To begin with, since

$$\begin{aligned} \|\mathbf{x} - \mathbf{a}'(\boldsymbol{\eta}) \alpha\|^2 &= \|\underline{\mathbf{x}} - \underline{\mathbf{a}}'(\boldsymbol{\eta}) \alpha\|^2 \\ &= \|\Pi_{\underline{\mathbf{a}}'(\boldsymbol{\eta})} (\underline{\mathbf{x}} - \underline{\mathbf{a}}'(\boldsymbol{\eta}) \alpha)\|^2 + \|\Pi_{\underline{\mathbf{a}}'(\boldsymbol{\eta})}^\perp (\underline{\mathbf{x}} - \underline{\mathbf{a}}'(\boldsymbol{\eta}) \alpha)\|^2 \\ &= \|\underline{\mathbf{a}}'(\boldsymbol{\eta}) (\hat{\alpha}_u(\boldsymbol{\eta}) - \alpha)\|^2 + \|\Pi_{\underline{\mathbf{a}}'(\boldsymbol{\eta})}^\perp \underline{\mathbf{x}}\|^2, \end{aligned} \quad (6)$$

where $\Pi_{\mathbf{A}} = \mathbf{A}(\mathbf{A}^H \mathbf{A})^{-1} \mathbf{A}^H$ and $\Pi_{\mathbf{A}}^\perp = \mathbf{I} - \Pi_{\mathbf{A}}$ are the orthogonal projectors over S and S^\perp , respectively. $S = \text{span}(\mathbf{A})$, with \mathbf{A} a matrix, is the linear span of the set of its column vectors. In addition,

$$\hat{\alpha}_u(\boldsymbol{\eta}) = \frac{\underline{\mathbf{a}}'(\boldsymbol{\eta})^T \underline{\mathbf{x}}}{\underline{\mathbf{a}}'(\boldsymbol{\eta})^T \underline{\mathbf{a}}'(\boldsymbol{\eta})} = \frac{\Re \{ \mathbf{a}'(\boldsymbol{\eta})^H \mathbf{x} \}}{\mathbf{a}'(\boldsymbol{\eta})^H \mathbf{a}'(\boldsymbol{\eta})},$$

denotes the unconstrained estimator of α [30], when the condition $\alpha > 0$ does not apply. The minimisation of the cost function in (6), yields

$$\left(\begin{array}{c} \hat{\boldsymbol{\eta}} \\ \hat{\alpha} \end{array} \right) = \arg \min_{\boldsymbol{\eta}, \alpha \geq 0} \left\{ (\hat{\alpha}_u(\boldsymbol{\eta}) - \alpha)^2 \|\mathbf{a}'(\boldsymbol{\eta})\|^2 + \|\Pi_{\underline{\mathbf{a}}'(\boldsymbol{\eta})}^\perp \underline{\mathbf{x}}\|^2 \right\}. \quad (7)$$

Since $\|\Pi_{\underline{\mathbf{a}}'(\boldsymbol{\eta})}^\perp \underline{\mathbf{x}}\|^2 = \|\underline{\mathbf{x}}\|^2 - \|\Pi_{\underline{\mathbf{a}}'(\boldsymbol{\eta})} \underline{\mathbf{x}}\|^2$, (7) leads to

$$\begin{aligned} \left(\begin{array}{c} \hat{\boldsymbol{\eta}} \\ \hat{\alpha} \end{array} \right) &= \arg \min_{\boldsymbol{\eta}, \alpha \geq 0} \left\{ \|\underline{\mathbf{x}}\|^2 + (\alpha - \hat{\alpha}_u(\boldsymbol{\eta}))^2 \|\mathbf{a}'(\boldsymbol{\eta})\|^2 \right. \\ &\quad \left. - \Re \left\{ \left(\frac{\mathbf{a}'(\boldsymbol{\eta})}{\|\mathbf{a}'(\boldsymbol{\eta})\|} \right)^H \mathbf{x} \right\}^2 \right\}. \end{aligned} \quad (8)$$

Since $d(\alpha - \hat{\alpha}_u(\boldsymbol{\eta}))^2 / d\alpha = 2(\alpha - \hat{\alpha}_u(\boldsymbol{\eta}))$, the following conditions apply for any given $\boldsymbol{\eta}$

$$\bullet \text{ if } \hat{\alpha}_u(\boldsymbol{\eta}) > 0 \text{ then } \begin{cases} \min_{\alpha \geq 0} \{ (\alpha - \hat{\alpha}_u(\boldsymbol{\eta}))^2 \} = 0 \\ \hat{\alpha}(\boldsymbol{\eta}) = \hat{\alpha}_u(\boldsymbol{\eta}) \end{cases}$$

and $(\hat{\alpha}(\boldsymbol{\eta}) - \hat{\alpha}_u(\boldsymbol{\eta}))^2 \|\mathbf{a}'(\boldsymbol{\eta})\|^2 = 0$.

$$\bullet \text{ if } \hat{\alpha}_u(\boldsymbol{\eta}) \leq 0 \text{ then } \begin{cases} \min_{\alpha \geq 0} \{ (\alpha - \hat{\alpha}_u(\boldsymbol{\eta}))^2 \} = \hat{\alpha}_u^2(\boldsymbol{\eta}) \\ \hat{\alpha}(\boldsymbol{\eta}) = 0 \end{cases}$$

and $(\hat{\alpha}(\boldsymbol{\eta}) - \hat{\alpha}_u(\boldsymbol{\eta}))^2 \|\mathbf{a}'(\boldsymbol{\eta})\|^2 = \Re \left\{ \frac{\mathbf{a}'(\boldsymbol{\eta})^H \mathbf{x}}{\|\mathbf{a}'(\boldsymbol{\eta})\|} \right\}^2$. Hence, $\forall \boldsymbol{\eta}$ the minimization of (8) w.r.t. α becomes

$$\begin{aligned} \min_{\alpha \geq 0} \left\{ \|\mathbf{x} - \mathbf{a}'(\boldsymbol{\eta}) \alpha\|^2 \right\} &= \\ \|\mathbf{x}\|^2 - \Re \left\{ \frac{\mathbf{a}'(\boldsymbol{\eta})^H \mathbf{x}}{\|\mathbf{a}'(\boldsymbol{\eta})\|} \right\}^2 &\mathbb{1}_{\Re \{ \mathbf{a}'(\boldsymbol{\eta})^H \mathbf{x} \} > 0}, \end{aligned} \quad (9)$$

where $\mathbb{1}_{\mathcal{D}}$ is the indicator function of subset \mathcal{D} of \mathbb{R} , and the solution of (8) w.r.t. $(\boldsymbol{\eta}, \alpha \geq 0)$ is then given by

$$\hat{\boldsymbol{\eta}} = \arg \min_{\{\boldsymbol{\eta} | \Re \{ \mathbf{a}'(\boldsymbol{\eta})^H \mathbf{x} \} > 0\}} \left\{ \|\mathbf{x}\|^2 - \Re \left\{ \frac{\mathbf{a}'(\boldsymbol{\eta})^H \mathbf{x}}{\|\mathbf{a}'(\boldsymbol{\eta})\|} \right\}^2 \right\}, \quad (10)$$

or equivalently,

$$\hat{\boldsymbol{\eta}} = \arg \max_{\{\boldsymbol{\eta} | \Re \{ \mathbf{a}'(\boldsymbol{\eta})^H \mathbf{x} \} > 0\}} \left\{ \Re \left\{ \frac{\mathbf{a}'(\boldsymbol{\eta})^H \mathbf{x}}{\|\mathbf{a}'(\boldsymbol{\eta})\|} \right\}^2 \right\}, \quad (11)$$

which for (3) becomes

$$\hat{\boldsymbol{\eta}} = \arg \max_{\{\boldsymbol{\eta} | \Re \{ e^{-j\varphi(\boldsymbol{\eta})} \mathbf{a}^H(\boldsymbol{\eta}) \mathbf{x} \} > 0\}} \left\{ \Re \left\{ \frac{e^{-j\varphi(\boldsymbol{\eta})} \mathbf{a}^H(\boldsymbol{\eta}) \mathbf{x}}{\|\mathbf{a}(\boldsymbol{\eta})\|} \right\}^2 \right\}. \quad (12)$$

3. CRAMÉR-RAO BOUND (CRB)

As shown in [31], in case of parameter inequality constraint the CRB is unchanged at a regular point, that is for $\alpha > 0$ the equality constraint is not active and is obtained through the inversion of the standard Fisher Information Matrix (FIM),

$$\mathbf{CRB}_{\boldsymbol{\epsilon}|\boldsymbol{\epsilon}}(\boldsymbol{\epsilon}^0) = \mathbf{F}(\boldsymbol{\epsilon}^0)^{-1}. \quad (13)$$

Given the gaussian properties of the signal model under study, the FIM is derived from the Slepian-Bangs formula [10] where $\underline{\mathbf{x}} \sim \mathcal{N}(\mathbf{m}_{\underline{\mathbf{x}}}(\boldsymbol{\epsilon}), \mathbf{C}_{\underline{\mathbf{x}}}(\boldsymbol{\epsilon}))$.

$$\begin{aligned} (\mathbf{F}(\boldsymbol{\epsilon}))_{k,l} &= \frac{\partial \mathbf{m}_{\underline{\mathbf{x}}}(\boldsymbol{\epsilon})^T}{\partial \epsilon_k} \mathbf{C}_{\underline{\mathbf{x}}}^{-1}(\boldsymbol{\epsilon}) \frac{\partial \mathbf{m}_{\underline{\mathbf{x}}}(\boldsymbol{\epsilon})}{\partial \epsilon_l} \\ &\quad + \frac{1}{2} \text{tr} \left(\mathbf{C}_{\underline{\mathbf{x}}}^{-1}(\boldsymbol{\epsilon}) \frac{\partial \mathbf{C}_{\underline{\mathbf{x}}}(\boldsymbol{\epsilon})}{\partial \epsilon_k} \mathbf{C}_{\underline{\mathbf{x}}}^{-1}(\boldsymbol{\epsilon}) \frac{\partial \mathbf{C}_{\underline{\mathbf{x}}}(\boldsymbol{\epsilon})}{\partial \epsilon_l} \right). \end{aligned} \quad (14)$$

The current study focuses on the derivation of $\mathbf{CRB}_{\boldsymbol{\eta}|\boldsymbol{\epsilon}}(\boldsymbol{\epsilon}) = \mathbf{F}_{\boldsymbol{\eta}|\boldsymbol{\epsilon}}^{-1}(\boldsymbol{\epsilon})$, which for the signal model proposed in (3) is given by [10]

$$\mathbf{F}_{\boldsymbol{\eta}|\boldsymbol{\epsilon}}(\boldsymbol{\epsilon}) = \frac{2\alpha^2}{\sigma_n^2} \boldsymbol{\Phi}(\boldsymbol{\eta}), \quad \boldsymbol{\Phi}(\boldsymbol{\eta}) = \left(\frac{\partial \underline{\mathbf{a}}'(\boldsymbol{\eta})}{\partial \boldsymbol{\eta}^T} \right)^T \Pi_{\underline{\mathbf{a}}'(\boldsymbol{\eta})}^\perp \frac{\partial \underline{\mathbf{a}}'(\boldsymbol{\eta})}{\partial \boldsymbol{\eta}^T} \quad (15)$$

The term $\Phi(\boldsymbol{\eta})$ can be also expressed as a function of \mathbf{a}' with aim to provide a closed-form expression for complex band-limited signals. Since

$$\Phi(\boldsymbol{\eta}) = \left(\frac{\partial \mathbf{a}'(\boldsymbol{\eta})}{\partial \boldsymbol{\eta}^T} \right)^T \frac{\partial \mathbf{a}'(\boldsymbol{\eta})}{\partial \boldsymbol{\eta}^T} - \frac{1}{\|\mathbf{a}'(\boldsymbol{\eta})\|^2} \left(\mathbf{a}'(\boldsymbol{\eta})^T \frac{\partial \mathbf{a}'(\boldsymbol{\eta})}{\partial \boldsymbol{\eta}^T} \right)^T \left(\mathbf{a}'(\boldsymbol{\eta})^T \frac{\partial \mathbf{a}'(\boldsymbol{\eta})}{\partial \boldsymbol{\eta}^T} \right) \quad (16)$$

and

$$\frac{\partial \mathbf{a}'(\boldsymbol{\eta})}{\partial \boldsymbol{\eta}^T} \frac{\partial \mathbf{a}'(\boldsymbol{\eta})}{\partial \boldsymbol{\eta}^T} = \Re \left\{ \frac{\partial \mathbf{a}'(\boldsymbol{\eta})}{\partial \boldsymbol{\eta}^T} \frac{\partial \mathbf{a}'(\boldsymbol{\eta})}{\partial \boldsymbol{\eta}^T} \right\}, \quad (17)$$

$$\mathbf{a}'(\boldsymbol{\eta})^T \frac{\partial \mathbf{a}'(\boldsymbol{\eta})}{\partial \boldsymbol{\eta}^T} = \Re \left\{ \mathbf{a}'(\boldsymbol{\eta})^H \frac{\partial \mathbf{a}'(\boldsymbol{\eta})}{\partial \boldsymbol{\eta}^T} \right\}. \quad (18)$$

Equation (16) can be rewritten as

$$\Phi(\boldsymbol{\eta}) = \Re \left\{ \left(\frac{\partial \mathbf{a}'(\boldsymbol{\eta})}{\partial \boldsymbol{\eta}^T} \right)^H \frac{\partial \mathbf{a}'(\boldsymbol{\eta})}{\partial \boldsymbol{\eta}^T} \right\} - \frac{1}{\|\mathbf{a}'(\boldsymbol{\eta})\|^2} \Re \left\{ \mathbf{a}'(\boldsymbol{\eta})^H \frac{\partial \mathbf{a}'(\boldsymbol{\eta})}{\partial \boldsymbol{\eta}^T} \right\}^T \Re \left\{ \mathbf{a}'(\boldsymbol{\eta})^H \frac{\partial \mathbf{a}'(\boldsymbol{\eta})}{\partial \boldsymbol{\eta}^T} \right\}. \quad (19)$$

The first element of (19) can be expanded as follows:

$$\begin{aligned} \Re \left\{ \left(\frac{\partial \mathbf{a}'(\boldsymbol{\eta})}{\partial \boldsymbol{\eta}^T} \right)^H \frac{\partial \mathbf{a}'(\boldsymbol{\eta})}{\partial \boldsymbol{\eta}^T} \right\} &= \Re \left\{ \left(\frac{\partial \mathbf{a}(\boldsymbol{\eta})}{\partial \boldsymbol{\eta}^T} \right)^H \frac{\partial \mathbf{a}(\boldsymbol{\eta})}{\partial \boldsymbol{\eta}^T} \right\} \\ &+ \Re \left\{ \left(\mathbf{a}(\boldsymbol{\eta}) \frac{\partial \varphi(\boldsymbol{\eta})}{\partial \boldsymbol{\eta}^T} \right)^H \left(\mathbf{a}(\boldsymbol{\eta}) \frac{\partial \varphi(\boldsymbol{\eta})}{\partial \boldsymbol{\eta}^T} \right) \right\} \\ &- \Im \left\{ \frac{\partial \mathbf{a}(\boldsymbol{\eta})}{\partial \boldsymbol{\eta}^T} \left(\mathbf{a}(\boldsymbol{\eta}) \frac{\partial \varphi(\boldsymbol{\eta})}{\partial \boldsymbol{\eta}^T} \right) \right. \\ &\left. - \left(\frac{\partial \mathbf{a}(\boldsymbol{\eta})}{\partial \boldsymbol{\eta}^T} \right)^H \left(\mathbf{a}(\boldsymbol{\eta}) \frac{\partial \varphi(\boldsymbol{\eta})}{\partial \boldsymbol{\eta}^T} \right) \right\} \end{aligned} \quad (20)$$

Note that

$$\begin{aligned} \Re \left\{ \mathbf{a}'(\boldsymbol{\eta})^H \frac{\partial \mathbf{a}'(\boldsymbol{\eta})}{\partial \boldsymbol{\eta}^T} \right\} &= \\ \Re \left\{ \mathbf{a}(\boldsymbol{\eta})^H \frac{\partial \mathbf{a}(\boldsymbol{\eta})}{\partial \boldsymbol{\eta}^T} \right\} - \Im \left\{ \mathbf{a}(\boldsymbol{\eta})^H \left(\mathbf{a}(\boldsymbol{\eta}) \frac{\partial \varphi(\boldsymbol{\eta})}{\partial \boldsymbol{\eta}^T} \right) \right\}, \end{aligned} \quad (21)$$

and (19) can be expressed as

$$\begin{aligned} \Phi(\boldsymbol{\eta}) &= \Re \left\{ \left(\frac{\partial \mathbf{a}(\boldsymbol{\eta})}{\partial \boldsymbol{\eta}^T} \right)^H \frac{\partial \mathbf{a}(\boldsymbol{\eta})}{\partial \boldsymbol{\eta}^T} \right\} \\ &+ \Re \left\{ \left(\mathbf{a}(\boldsymbol{\eta}) \frac{\partial \varphi(\boldsymbol{\eta})}{\partial \boldsymbol{\eta}^T} \right)^H \left(\mathbf{a}(\boldsymbol{\eta}) \frac{\partial \varphi(\boldsymbol{\eta})}{\partial \boldsymbol{\eta}^T} \right) \right\} \\ &- \Im \left\{ \frac{\partial \mathbf{a}(\boldsymbol{\eta})}{\partial \boldsymbol{\eta}^T} \left(\mathbf{a}(\boldsymbol{\eta}) \frac{\partial \varphi(\boldsymbol{\eta})}{\partial \boldsymbol{\eta}^T} \right) - \left(\frac{\partial \mathbf{a}(\boldsymbol{\eta})}{\partial \boldsymbol{\eta}^T} \right)^H \left(\mathbf{a}(\boldsymbol{\eta}) \frac{\partial \varphi(\boldsymbol{\eta})}{\partial \boldsymbol{\eta}^T} \right) \right\} \\ &+ \frac{1}{\|\mathbf{a}(\boldsymbol{\eta})\|^2} \left(\Re \left\{ \mathbf{a}(\boldsymbol{\eta})^H \frac{\partial \mathbf{a}(\boldsymbol{\eta})}{\partial \boldsymbol{\eta}^T} \right\} - \Im \left\{ \mathbf{a}(\boldsymbol{\eta})^H \left(\mathbf{a}(\boldsymbol{\eta}) \frac{\partial \varphi(\boldsymbol{\eta})}{\partial \boldsymbol{\eta}^T} \right) \right\} \right)^T \\ &\times \left(\Re \left\{ \mathbf{a}(\boldsymbol{\eta})^H \frac{\partial \mathbf{a}(\boldsymbol{\eta})}{\partial \boldsymbol{\eta}^T} \right\} - \Im \left\{ \mathbf{a}(\boldsymbol{\eta})^H \left(\mathbf{a}(\boldsymbol{\eta}) \frac{\partial \varphi(\boldsymbol{\eta})}{\partial \boldsymbol{\eta}^T} \right) \right\} \right). \end{aligned} \quad (22)$$

Since $\varphi(\boldsymbol{\eta}) = -2\pi f_c(\tau + b(t - \tau))$ and $\mathbf{a}(\boldsymbol{\eta}) = a(t - \tau)$, we can compute the following terms:

$$\left(\frac{\partial \mathbf{a}(\boldsymbol{\eta})}{\partial \boldsymbol{\eta}} \right) = \begin{pmatrix} -a^{(1)}(t - \tau) \\ 0 \end{pmatrix}, \quad \left(\frac{\partial \varphi(\boldsymbol{\eta})}{\partial b} \right) = - \begin{pmatrix} 2\pi f_c(1 - b) \\ 2\pi f_c(t - \tau) \end{pmatrix}, \quad (23)$$

with $a^{(1)}(t) = \frac{\partial a(t)}{\partial t}$.

3.1. CRB for band-limited signals

Assuming a band-limited signal, we derive a closed-form expression for (22). According to the Nyquist-Shannon theorem,

$$\begin{aligned} \lim_{(N'_1, N'_2) \rightarrow (-\infty, +\infty)} T_s \left\| \frac{\partial \mathbf{a}(\boldsymbol{\eta})}{\partial \boldsymbol{\eta}} \right\|^2 &= \int_{-\infty}^{+\infty} \left| \frac{\partial a(t - \tau)}{\partial \tau} \right|^2 dt = W_{3,3}, \\ \lim_{(N'_1, N'_2) \rightarrow (-\infty, +\infty)} T_s \|\mathbf{a}(\boldsymbol{\eta})\|^2 &= \int_{-\infty}^{+\infty} |a(t - \tau)|^2 dt = w_1, \\ \lim_{(N'_1, N'_2) \rightarrow (-\infty, +\infty)} T_s \mathbf{a}(\boldsymbol{\eta})^H \frac{\partial \mathbf{a}(\boldsymbol{\eta})}{\partial \boldsymbol{\eta}} &= \\ \int_{-\infty}^{+\infty} a(t - \tau)^* \frac{\partial a(t - \tau)}{\partial \tau} dt &= w_3, \\ \lim_{(N'_1, N'_2) \rightarrow (-\infty, +\infty)} T_s \left(\mathbf{a}(\boldsymbol{\eta}) \frac{\partial \varphi(\boldsymbol{\eta})}{\partial \boldsymbol{\eta}} \right)^H \left(\mathbf{a}(\boldsymbol{\eta}) \frac{\partial \varphi(\boldsymbol{\eta})}{\partial b} \right) &= \\ (1 - b)(2\pi f_c)^2 \int_{-\infty}^{+\infty} (t - \tau) |a(t - \tau)|^2 dt &= (1 - b)(2\pi f_c)^2 w_2, \\ \lim_{(N'_1, N'_2) \rightarrow (-\infty, +\infty)} T_s \left(\mathbf{a}(\boldsymbol{\eta}) \frac{\partial \varphi(\boldsymbol{\eta})}{\partial b} \right)^H \left(\mathbf{a}(\boldsymbol{\eta}) \frac{\partial \varphi(\boldsymbol{\eta})}{\partial b} \right) &= \\ (2\pi f_c)^2 \int_{-\infty}^{+\infty} (t - \tau)^2 |a(t - \tau)|^2 dt &= (2\pi f_c)^2 W_{2,2}, \\ \lim_{(N'_1, N'_2) \rightarrow (-\infty, +\infty)} T_s \left(\frac{\partial \mathbf{a}(\boldsymbol{\eta})}{\partial \boldsymbol{\eta}} \right)^H \left(\mathbf{a}(\boldsymbol{\eta}) \frac{\partial \varphi(\boldsymbol{\eta})}{\partial b} \right) &= \\ (2\pi f_c) \int_{-\infty}^{+\infty} (t - \tau) \frac{\partial a^*(t - \tau)}{\partial \tau} a(t - \tau) dt &= (2\pi f_c) \varpi^*. \end{aligned}$$

Then,

$$\lim_{(N'_1, N'_2) \rightarrow (-\infty, \infty)} \Phi(\boldsymbol{\eta}) = F_s \begin{bmatrix} \Phi_{1,1} & \Phi_{1,2} \\ \Phi_{2,1} & \Phi_{2,2} \end{bmatrix},$$

with

$$\begin{aligned} \Phi_{1,1} &= W_{3,3} + \Re \{w_1\} (1 - b)^2 w_c^2 \\ &- \frac{\Re \{w_3\}^2}{w_1} + \Im \{w_3\} (1 - b) 2w_c, \\ \Phi_{1,2} &= \Phi_{2,1}^* = \Re \{w_2\} (1 - b) w_c^2 \\ &- \frac{\Re \{w_3\} \Im \{w_2\}}{w_1} w_c - \Im \{w_3^*\} w_c, \\ \Phi_{2,2} &= W_{2,2} w_c^2 - \frac{\Im \{w_2\}^2}{w_1} w_c^2. \end{aligned} \quad (24)$$

and $w_c = 2\pi f_c$. After some algebraic manipulations, w_1 , w_2 , w_3 , ϖ , $W_{2,2}$ and $W_{3,3}$ can be reformulated as follows for $-N_1 \leq n, n' \leq N_2$,

$$\begin{aligned} w_1 &= \frac{1}{F_s} \mathbf{a}^H \mathbf{a}, \quad w_2 = \frac{1}{F_s^2} \mathbf{a}^H \mathbf{D} \mathbf{a}, \quad w_3 = \mathbf{a}^H \boldsymbol{\Lambda} \mathbf{a}, \\ W_{2,2} &= \frac{1}{F_s^3} \mathbf{a}^H \mathbf{D}^2 \mathbf{a}, \quad \varpi = \frac{1}{F_s} \mathbf{a}^H \mathbf{D} \boldsymbol{\Lambda} \mathbf{a}, \quad W_{3,3} = F_s \mathbf{a}^H \mathbf{V} \mathbf{a}, \end{aligned}$$

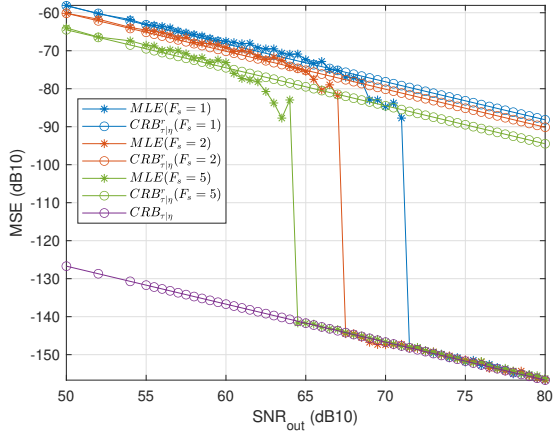


Fig. 1: $CRB_{\tau|\eta}(\epsilon)$ (22), $CRB_{\tau|\eta}^r(\epsilon)$ [28] and MLE (8) computed for $F_s = [1, 2, 5]$.

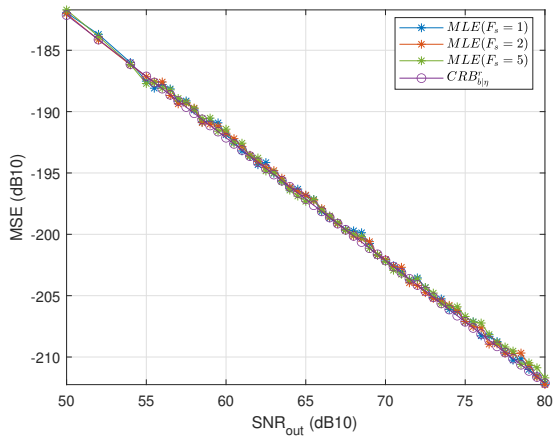


Fig. 2: $CRB_{b|\eta}(\epsilon)$ (22) and MLE (8) computed for $F_s = [1, 2, 5]$.

with $\mathbf{D} = \text{diag}(N_1, \dots, N_2)$ and

$$(\mathbf{A})_{n,n'} = \begin{cases} n' \neq n : \frac{(-1)^{|n-n'|}}{n-n'} \\ n' = n : 0 \end{cases},$$

$$(\mathbf{V})_{n,n'} = \begin{cases} n' \neq n : (-1)^{|n-n'|} \frac{2}{(n-n')^2} \\ n' = n : \frac{\pi^2}{3} \end{cases}$$

4. SIMULATIONS

This section describes the simulation process to validate both the MLE and CRB expressions of the time delay and Doppler derived in sections 2.1 and 3, respectively. The goal is to illustrate the MSE of the MLE as a function of the SNR at the output of the match filter SNR_{out} . Higher values of SNR_{out} are expected to benefit the estimation performance of the MLE, up to an optimal value defined by the CRB.

The testing setup employs one code period of a GPS L1 C/A signal [29], composed by a periodic BPSK Gold Code of 1023 chips,

with a time period of $T_c = 1 \text{ ms}$ and a carrier frequency of $f_c = 1575.42 \text{ MHz}$. We set a Doppler frequency of 500 Hz and we set the integration time to 1 ms . The SNR at the output of the MLE estimator (a.k.a matched filter [10]) for the true parameter $\boldsymbol{\eta}^0$ can be defined as follows:

$$SNR_{out} = \frac{\Re \left\{ \frac{e^{-j\varphi(\boldsymbol{\eta})} \mathbf{a}(\boldsymbol{\eta})^H}{\|\mathbf{a}(\boldsymbol{\eta})\|} \left(\alpha^0 \mathbf{a}(\boldsymbol{\eta}^0) e^{-j\varphi(\boldsymbol{\eta}^0)} \right) \right\}^2}{E \left[\Re \left\{ \frac{e^{-j\varphi(\boldsymbol{\eta})} \mathbf{a}(\boldsymbol{\eta})^H \mathbf{n}}{\|\mathbf{a}(\boldsymbol{\eta})\|} \right\}^2 \right]} \Bigg|_{\boldsymbol{\eta}=\boldsymbol{\eta}^0}$$

$$= \frac{(\alpha^0)^2 \|\mathbf{a}(\boldsymbol{\eta}^0)\|^2}{\frac{(\sigma_n^0)^2}{2}} = \frac{2 \|\mathbf{a}\|^2}{(\sigma_n^0)^2} (\alpha^0)^2. \quad (25)$$

and (15) becomes $\mathbf{F}_{\boldsymbol{\eta}|\epsilon}(\boldsymbol{\epsilon}) = \frac{SNR_{out}}{\mathbf{a}^H \mathbf{a}} \boldsymbol{\Phi}(\boldsymbol{\eta})$.

Figs. 1 and 2, illustrate both time-delay and doppler MSE from their MLEs, along with the CRB expressions derived in section 3. Such equations are verified employing 1000 Monte-Carlo simulations for $F_s = 1, 2, 5 \text{ MHz}$. In addition, the CRB expression derived in [28] is included as well (which we refer to as $CRB_{\tau|\eta}^r(\epsilon)$) for comparison. As a quick reminder, the signal model employed in the present study leaves the signal's carrier-phase component out of α , as opposed to [28], since in this case it is of interest to assess its effect on performance.

From Fig. 1, we can see that the MSE of the MLE for the time delay converges asymptotically to the derived CRB, which validates both the MLE and the closed-form $CRB_{\tau|\eta}(\epsilon)$ expressions provided. Similarly, in Fig. 2, it can be observed that the MSE of the Doppler's MSE converges to the derived $CRB_{b|\eta}(\epsilon)$. In the case of the time delay estimation, two interesting points can be drawn. Firstly, it is observed that increasing the sampling frequency benefits the system threshold. That is, increasing F_s reduces the amount of SNR_{out} required for convergence to the bound. Secondly, in the region before the convergence, there is a SNR_{out} interval in which the derived MLE behaves as the classical unconstrained MLE, since the MSE of the MLE converges to the bound derived in [28].

5. CONCLUSION

The goal of this paper was to define the optimal estimation performance of the time delay and Doppler for a particular CSM, which takes into account the carrier-phase of the signal. This assessment was structured in four sections. Section 2 presents the signal model employed, including the associated MLE for both time-delay and Doppler parameters in subsection 2.1. Then, section 3 provides a step-by-step derivation process of the CRB defining the theoretical accuracy limits for both MLEs. Section 4 validates the previous expressions by running Monte Carlo simulations using a GPS L1 C/A signal, which showed the convergence of both MLEs to their respective CRBs and we compare the results with respect to other model proposed in the state of the art. This contribution provides an estimation tool which could be used to assess the optimal performance limits in the estimation of the time-delay and Doppler for new operational systems based on phase measurements.

6. REFERENCES

- [1] D. A. Swick, "A Review of Wideband Ambiguity Functions," Tech. Rep. 6994, Naval Res. Lab., Washington DC, 1969.
- [2] H. L. Van Trees, *Detection, Estimation, and Modulation Theory, Part III: Radar – Sonar Signal Processing and Gaussian Signals in Noise*, J. Wiley & Sons, 2001.

- [3] U. Mengali and A. N. D'Andrea, *Synchronization Techniques for Digital Receivers*, Plenum Press, New York, USA, 1997.
- [4] H. L. Van Trees, *Optimum Array Processing*, Wiley-Interscience, New-York, 2002.
- [5] D. W. Ricker, *Echo Signal Processing*, Kluwer Academic, Springer, New York, USA, 2003.
- [6] J. Chen, Y. Huang, and J. Benesty, "Time delay estimation," in *Audio Signal Processing for Next-Generation Multimedia Communication Systems*, Y. Huang and J. Benesty, Eds., chapter 8, pp. 197–227. Springer, Boston, MA, USA, 2004.
- [7] B. C. Levy, *Principles of Signal Detection and Parameter Estimation*, Springer, 2008.
- [8] F. Bouchereau D. Munoz, C. Vargas, and R. Enriquez, *Position Location Techniques and Applications*, Academic Press, Oxford, GB, 2009.
- [9] J. Yan et al., "Review of range-based positioning algorithms," *IEEE Trans. Aerosp. Electron. Syst.*, vol. 28, no. 8, pp. 2–27, Aug. 2013.
- [10] S. M. Kay, *Fundamentals of Statistical Signal Processing: Estimation Theory*, Prentice-Hall, Englewood Cliffs, New Jersey, USA, 1993.
- [11] H. L. Van Trees and K. L. Bell, Eds., *Bayesian Bounds for Parameter Estimation and Nonlinear Filtering/Tracking*, Wiley/IEEE Press, NY, USA, 2007.
- [12] P. Stoica and A. Nehorai, "Performances study of conditional and unconditional direction of arrival estimation," *IEEE Trans. Acoust., Speech, Signal Process.*, vol. 38, no. 10, pp. 1783–1795, Oct. 1990.
- [13] A. Renaux, P. Forster, E. Chaumette, and P. Larzabal, "On the high-SNR conditional maximum-likelihood estimator full statistical characterization," *IEEE Trans. Signal Process.*, vol. 54, no. 12, pp. 4840–4843, Dec. 2006.
- [14] Q. Jin, K. M. Wong, and Z.-Q. Luo, "The Estimation of Time Delay and Doppler Stretch of Wideband Signals," *IEEE Trans. Signal Process.*, vol. 43, no. 4, pp. 904–916, April 1995.
- [15] A. Dogandzic and A. Nehorai, "Cramér-Rao bounds for estimating range, velocity, and direction with an active array," *IEEE Trans. Signal Process.*, vol. 49, no. 6, pp. 1122–1137, June 2001.
- [16] N. Noels, H. Wymeersch, H. Steendam, and M. Moeneclaey, "True Cramér-Rao bound for timing recovery from a bandlimited linearly modulated waveform with unknown carrier phase and frequency," *IEEE Trans. on Communications*, vol. 52, no. 3, pp. 473–483, March 2004.
- [17] Y. Shangfu W. He-Wen and W. Qun, "Influence of random carrier phase on true cramér-rao lower bound for time delay estimation," in *Proc. of the IEEE Intl. Conf. on Acoustics, Speech and Signal Processing (ICASSP)*, Honolulu, USA, April 2007.
- [18] J. Johnson and M. Fowler, "Cramér-rao lower bound on doppler frequency of coherent pulse trains," in *Proc. of the IEEE Intl. Conf. on Acoustics, Speech and Signal Processing (ICASSP)*, Las Vegas, USA, March 2008.
- [19] P. Closas, C. Fernández-Prades, and J. A. Fernández-Rubio, "Cramér-Rao Bound Analysis of Positioning Approaches in GNSS Receivers," *IEEE Trans. on Signal Processing*, vol. 57, no. 10, pp. 3775–3786, Nov. 2009.
- [20] T. Zhao and T. Huang, "Cramér-Rao lower bounds for the joint delay-doppler estimation of an extended target," *IEEE Trans. Signal Process.*, vol. 64, no. 6, pp. 1562–1573, March 2016.
- [21] Y. Chen and R. S. Blum, "On the Impact of Unknown Signals on Delay, Doppler, Amplitude, and Phase Parameter Estimation," *IEEE Trans. Signal Process.*, vol. 67, no. 2, pp. 431–443, Jan. 2019.
- [22] D. Medina, J. Vilà-Valls, E. Chaumette, François Vincent, and P. Closas, "Cramér-Rao bound for a mixture of real- and integer-valued parameter vectors and its application to the linear regression model," *Signal Processing*, vol. 179, pp. 107792, 2021.
- [23] P. C. Ching X.X. Niu and Y.T. Chan, "Wavelet based approach for joint time delay and Doppler stretch measurements," *IEEE Trans. Aerosp. Electron. Syst.*, vol. 35, no. 3, pp. 1111–1119, July 1999.
- [24] P. Das, J. Vilà-Valls, F. Vincent, L. Davain, and E. Chaumette, "A New Compact Delay, Doppler Stretch and Phase Estimation CRB with a Band-Limited Signal for GenE. Remote Sensing Applications," *Remote Sensing*, vol. 12, no. 18, pp. 2913, Sep. 2020.
- [25] C. Lubeigt, L. Ortega, J. Vilà-Valls, L. Lestarquit, and E. Chaumette, "Joint delay-doppler estimation performance in a dual source context," *Remote Sensing*, vol. 12, no. 23, 2020.
- [26] H. McPhee, L. Ortega, J. Vilà-Valls, and E. Chaumette, "Accounting for acceleration—signal parameters estimation performance limits in high dynamics applications," *IEEE Transactions on Aerospace and Electronic Systems*, vol. 59, no. 1, pp. 610–622, 2023.
- [27] A. Bartov and H. Messer, "Lower bound on the achievable DSP performance for localizing step-like continuous signals in noise," *IEEE Trans. Signal Process.*, vol. 46, no. 8, pp. 2195–2201, Aug. 1998.
- [28] D. Medina, L. Ortega, J. Vilà-Valls, P. Closas, François Vincent, and E. Chaumette, "Compact CRB for Delay, Doppler, and Phase Estimation – Application to GNSS SPP and RTK Performance Characterisation," *IET Radar, Sonar & Navigation*, vol. 14, no. 10, pp. 1537–1549, 2020.
- [29] P. Das, L. Ortega, J. Vilà-Valls, F. Vincent, E. Chaumette, and Loïc Davain, "Performance limits of gnss code-based precise positioning: Gps, galileo & meta-signals," *Sensors*, vol. 20, no. 8, pp. 2196, 2020.
- [30] B. Ottersten, M. Viberg, P. Stoica, and A. Nehorai, "Exact and Large Sample Maximum Likelihood Techniques for Parameter Estimation and Detection in Array Processing," in *Radar Array Processing*, S. Haykin, J. Litva, and T. J. Shepherd, Eds., chapter 4, pp. 99–151. Springer-Verlag, Heidelberg, 1993.
- [31] J. D Gorman and A. O Hero, "Lower bounds for parametric estimation with constraints," *IEEE Transactions on Information Theory*, vol. 36, no. 6, pp. 1285–1301, 1990.